

[illegible]

STIC
LECTE
NOV 12 1992
D
E



DTIC QUALITY INSPECTED 4

Accession For	
NTIS CRASH	<input checked="" type="checkbox"/>
DTIC TAG	<input checked="" type="checkbox"/>
Unannounced	<input type="checkbox"/>
Justification	
By	
Distribution	
Availability Codes	
Dist	Avail. and/or Sec. di
A-1	20

Evolution and advection of solar mesogranulation

Richard Muller*, Hervé Auffret*, Thierry Roudier†, Jean Vigneau‡, George W. Simon‡, Zoe Frank§, Richard A. Shine§ & Alan M. Title§

* Observatoire du Pic du Midi, 65200 Bagneres de Bigorre, France

† Observatoire du Pic du Midi, 31400 Toulouse, France

‡ Phillips Laboratory (AFSC), National Solar Observatory, Sunspot, New Mexico 88349, USA

§ Lockheed Palo Alto Research Laboratory, Palo Alto, California 94304, USA

GRANULAR structure on the Sun's surface, with a typical scale of 1–2 Mm, has been known since 1800, and one hundred years ago, with the first observations by spectroheliograph^{1,2}, a mesh-like bright network was found with a characteristic scale of 30 Mm (40"). This pattern was found, thirty years ago, to be coincident with close-packed convective cells ('supergranulation') revealed by Doppler observations^{3–5} to be nestling inside the bright network. More recently^{6,7} an intermediate 'mesogranular' structure was found, with a characteristic scale of 3–10 Mm. We have obtained a three-hour sequence of observations at the Pic du Midi observatory which shows the evolution of mesogranules from appearance to disappearance with unprecedented clarity. We see that the supergranules, which are known to carry along (advect) the granules with their convective motion, also advect the mesogranules to their boundaries. This process controls the evolution and disappearance of mesogranules.

The origin of the bright network first seen by Hale¹ and Deslandres² was not explained until the observation of convective cells inside the mesh structure. It was then argued³ that convection sweeps magnetic flux to the boundaries of the cells and concentrates it there, enhancing local heating of the upper photosphere and chromosphere. A half-hour movie of the mesogranular structure made using the Solar Optical Universal

Photometer (SOLP) instrument on board the 1985 Spacelab 2 space shuttle flight⁸ first revealed the complexity of the surface flow patterns, which are evidence for subphotospheric convection. The SOLP movies showed that granules are advected by the larger-scale convective flows, and thus could be used as tracers of their motions. Horizontal flow maps produced by correlation tracking of the granules confirmed the existence of mesogranules and greatly improved our understanding of the intimate relation between supergranules and magnetic structures⁹. Unfortunately the SOLP movie lasted only 27.5 min (because of the day-night cycle of the space shuttle's equatorial near-Earth orbit), much less than the lifetime of supergranules and mesogranules, and its spatial resolution was limited by the relatively small size (30 cm) of the telescope aperture. Here we report recent observations taken at the Observatoire du Pic du Midi (French Pyrenees) with a 50-cm telescope, in a continuous 3-h sequence. The observations are nearly diffraction-limited.

Unfortunately, even the best ground-based observations are blurred and distorted by 'seeing' (turbulence in the Earth's atmosphere). To remove local image distortions, sophisticated algorithms have recently been developed to align and destretch sequential images¹⁰. In addition, the entire solar atmosphere oscillates with a range of periods centred around 5 min. These periods are sufficiently close to the lifetime of the granulation pattern (~10 min) to complicate studies of convective flows. But because these oscillations have a well defined dispersion relation, and the phase velocity of the waves generally is higher than the sound speed, three-dimensional Fourier filtering in space-time¹¹ is effective in removing them from a movie. After elimination of the seeing distortions and solar wave motions, local correlation tracking^{9,10} (a technique for measuring motions of the granules) on the time-series of images determines the horizontal velocity field. Because the majority of convective flow patterns visible at the surface are horizontal, measurements with the commonly used Doppler technique are ineffective, and local correlation tracking provides the only method for the study of such motions near the centre of the solar disk. This procedure yields the average velocity of the intensity pattern inside the

tracking window (whose full width at half maximum is usually 1–3 Mm, and thus represents the motion of 2–10 granules).

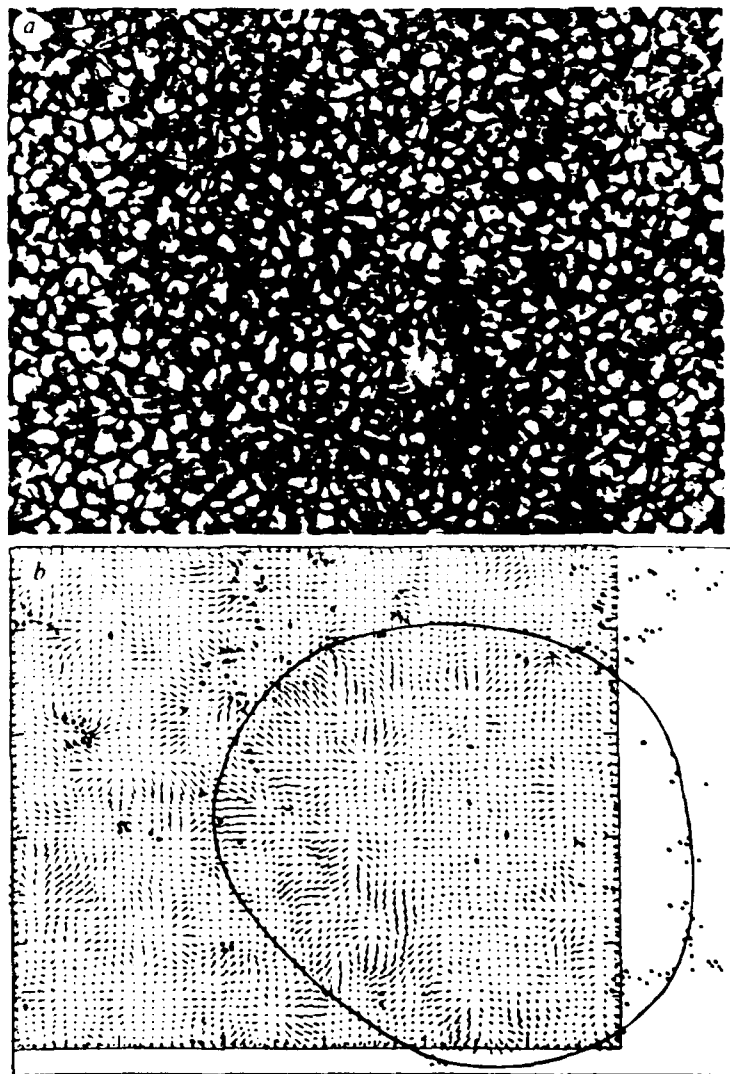
The data were collected on film with a camera that took bursts of frames every 20 s. They were obtained on 20 September 1988, in a $70'' \times 100''$ area of the Sun near disk centre. A $67'' \times 67''$ portion of the best frame from each burst is first digitized using a $1,024 \times 1,024$ digital CCD camera and then destretched, space-time filtered, and correlation tracked. Because of solar rotation, each of the digitized images covers a slightly different area; thus our analysis is restricted to an area of $58'' \times 48''$ common to all the frames. The extremely high quality of the images is confirmed by the appearance of numerous network bright points (NBPs) which are only visible when the resolution is $0.3''$ or better. The NBPs are relatively short-lived bright areas in the surface which are cospatial with magnetic flux tubes^{11,12}, and can thus be used to infer the locations of magnetic structures in an image of the surface. In Fig. 1a we show a $70'' \times 50''$ section of one of these granulation images and identify several of the prominent NBPs by three converging short lines. (Such photos contain many small transient bright features; NBPs are defined to be those with lifetimes exceeding 7 min.)

In Fig. 1b we show the flow vectors derived from correlation tracking a $58'' \times 48''$ portion of Fig. 1a. All the NBPs observed during the first 20 min of the observing sequence are superposed on the vector plot. The outer rectangle delineates the area included in Fig. 1a. The NBPs, which extend beyond the digit-

ized area of the image, and the flow vectors permit us to outline roughly the boundary of a supergranule, shown as a hand-drawn oval. The supergranule is ~ 30 Mm ($40''$) across. We identify mesogranules as the centres of diverging flow vectors (sources) in Fig. 1b. We have calculated the effect of the flow vectors on an initially uniform distribution of 'corks' (test particles used to simulate magnetic flux tubes), and confirm earlier results^{8,13} that all corks eventually end up in the supergranular network, many of them at or near the observed NBPs. Cork patterns calculated from velocity maps separated by 2–3 hours are almost unchanged on the scale of 1 supergranule during this time interval.

At the smaller scale of mesogranules, however, these patterns are very different after two hours, implying considerable changes in the mesogranulation. To study the characteristics of mesogranule evolution during the three hours in more detail, we show in the left column of Fig. 2 four flow maps averaged over 17 min at 54-min intervals. (The averaging time must be long enough to reduce measurement noise but short compared to mesogranule lifetimes.) The velocity vectors $\mathbf{v} = (u, v)$ are superposed on a grey-scale image of the divergence $\nabla = \partial u / \partial x + \partial v / \partial y$ computed from these flows. Bright areas (where the vectors point outward, that is, diverge) correspond to sources; in the dark areas (sinks), arrows point inward (converge). In the right column of Fig. 2 is a two-level contour map of the divergence. The levels displayed were chosen to

FIG. 1 a Typical image of solar granulation obtained in the high-quality 3-h data set of 20 September 1988. Area is $70'' \times 50''$. Converging lines point to examples of NBPs (see text). b Flow vectors in a $58'' \times 48''$ section of the larger area of a (outer rectangle). Line marks supergranule boundary. Black dots are loci of NBPs.



correspond to the brightest and darkest features in the grey-scale images. Many of the positive divergence contours (solid lines) represent mesogranules. The dashed-line contours are in regions of converging flows. These form a more connected, linear, pattern than do the positive contours. The supergranule boundary clearly lies largely in such converging regions. The $58'' \times 48''$ area covered by Fig. 2 is exactly cospatial with the vector map of Fig. 1b. Time increases from top to bottom. We have labelled 10 mesogranules in Fig. 2 to describe more easily various aspects of their evolution. Mesogranules 2, 5, 11, 16, 22 and 26 all illustrate our most interesting new result: the advection of mesogranules toward the supergranule boundary. This motion is evident, especially when the mesogranules are located away from the supergranule centre. The translational velocities range from zero to 0.7 km s^{-1} , with a mean velocity of $0.3\text{--}0.4 \text{ km s}^{-1}$.

This is consistent with the horizontal velocity of supergranules obtained from Dopplergrams¹. Asymmetry in the vector pattern also suggests a mesogranular flow toward the boundary: velocity arrows are longer on one side of the mesogranules, indicating motions towards the supergranular boundary. There are 5–10 well established diverging regions in this portion of the supergranule cell at any time, so that the entire supergranule contains perhaps a dozen such outflows. Visual inspection suggests two types of mesogranular motion: those mesogranules such as 1 that form near the supergranule centre move randomly, whereas those that emerge closer to a supergranule boundary drift towards that boundary, when they reach it, they collapse and disappear. Examples of disappearance are 15, 16 and 22, whereas mesogranules 3, 9 and 11 appear during the run. On average, two of these sources appear or disappear each hour in

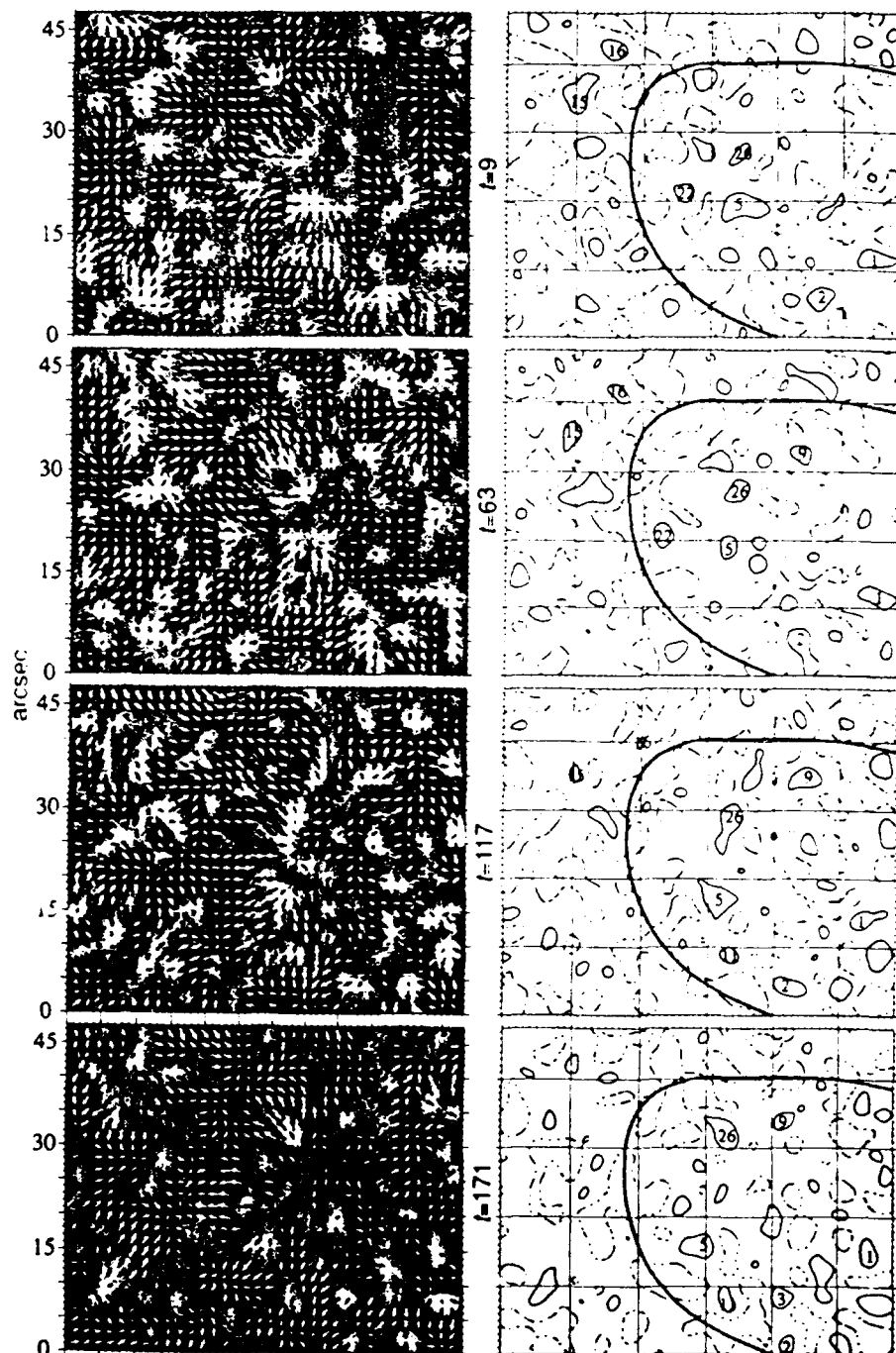


FIG. 2 Left column: velocity vectors superposed on grey-scale images of the flow divergence at 54-min intervals during the sequence. Right column: contours of the divergence include 10 examples of mesogranule evolution as described in the text. Same $58'' \times 48''$ area as in Fig. 1b; hand-drawn lines again show boundary of supergranule.

the area studied, and four of the labelled mesogranules (1, 2, 5 and 26) are present throughout the run. Results from this small data sample imply a mesogranule lifetime of ~ 3 h. As some mesogranules suffer premature deaths when they collide with the supergranule boundary, their intrinsic lifetimes may be somewhat longer¹⁴. A close look at the four vector images in Fig. 2 shows that the predominant arrow pattern near the supergranule boundary represents a long-lived flow toward that boundary, one that hardly changes in three hours. In fact it is well known¹⁵ that the supergranule lifetime is about a day or longer. Although we have illustrated our results with only four time steps, the actual analysis involved a detailed study of 78 such images made every two minutes over the 3-h sequence.

The mesogranular pattern is thus more dynamic and irregular than that of supergranules. Part of this difference is due to the shorter lifetimes and smaller sizes of the mesogranules, but most of it probably results from fluctuations of their flow fields due to exploding granules¹⁶ (bright granules that develop a dark centre and then expand radially as a bright annulus until they burst into fragments) within them, horizontal advection by the supergranular flows, and finally their collisions with the supergranule boundary. What, then, is the nature of the mesogranulation? It has been suggested recently¹⁷ that granules and supergranules are the two basic scales in the Sun's convection zone, whereas the mesogranules occur as transient secondary features within the supergranule, similar to convection patterns observed in the laboratory^{18,19} and in theoretical models²⁰.

Our analysis of the Pic du Midi movie has revealed a hierarchy of advecting convective flow patterns at the surface of the Sun. We have confirmed that granules move in the flow fields of mesogranules and have discovered that the mesogranules, in turn, are advected by the still-larger supergranules. As this pattern of motions evolves with time in a statistically random fashion, it drags along bits of magnetic flux that appear at the Sun's surface. This diffusion process first concentrates the flux into the supergranular network²¹, but as the supergranules themselves evolve over days and weeks, magnetic field will be redistributed over much larger regions of the Sun. In conjunction with the Sun's poleward-moving meridional velocity field, this mechanism may be partially responsible for large-scale magnetic field transport over the Sun during the solar cycle²².

Recent kinematic modelling²³ of these motions has considerably clarified our understanding of the relative roles of granules, exploding granules, mesogranules and supergranules in the evolution of solar surface flow patterns, but to understand these phenomena in detail will require theoretical modelling of three-dimensional compressible convection, a difficult area in which considerable progress is now being made^{24,25}. The Sun continues to be a unique laboratory for the study of magnetohydrodynamic convection.

21. Simon, G. W., Title, A. M. & Weiss, N. O. *Astrophys. J.* **375**, 775-788 (1991).
22. Spruit, H. C., Nordlund, Å. & Title, A. M. *Ann. Rev. Astr. Astrophys.* **28**, 263-301 (1990).
23. Stein, R. F. & Nordlund, Å. *Astrophys. J.* **342**, L95-L98 (1989).
24. Cattaneo, F., Brummell, N. H., Toomre, J., Malagoli, A. & Hurlburt, N. E. *Astrophys. J.* **370**, 282-291 (1991).

ACKNOWLEDGEMENTS. We thank P. Brandt, J. Toomre and N. Weiss for discussion. H.A.R.M. and J.V. thank the US Air Force Office of Scientific Research and its Window on Science Program, the French Ministère des Affaires Étrangères and the Groupe de Recherche du CNRS 'Magnetisme dans les Étoiles de Type Solaire' for financial support and also acknowledge the kind hospitality of the Lockheed Palo Alto Research Laboratory and the National Solar Observatory. This project was partially supported by NASA and the NSF.

Received 13 September 1991; accepted 14 February 1992

1. Hale, G. *Astr. Astrophys.* **11**, 407-417 (1892).
2. Desandres, H. C. R. *Acad. Sci. Paris* **118**, 842-844 (1894).
3. Hale, A. *Mon. Not. R. Astr. Soc.* **116**, 38-55 (1917).
4. Leighton, R. B., Hayes, R. W. & Simon, G. W. *Astrophys. J.* **135**, 474-499 (1962).
5. Simon, G. W. & Leighton, R. B. *Astrophys. J.* **140**, 110-1147 (1964).
6. November, L. J., Toomre, J., Gebbie, K. & Simon, G. W. *Astrophys. J.* **245**, L123-L126 (1981).
7. Title, A. M. et al. *Adv. Space Res.* **8**, 253-262 (1986).
8. Simon, G. W. et al. *Astrophys. J.* **327**, 964-967 (1988).
9. November, L. J. *Appl. Optics* **25**, 392-397 (1986).
10. November, L. J. & Simon, G. W. *Astrophys. J.* **333**, 427-442 (1988).
11. Stenflo, J. O. & Harvey, J. W. *Solar Phys.* **95**, 99-118 (1985).
12. Muller, R. *Solar Phys.* **100**, 237-255 (1985).
13. Title, A. M., Shine, R. A., Tarbell, T. D., Topka, K. P. & Scherrer, G. B. in *Solar Photosphere Structure: Convection and Magnetic Fields* (IAU Symp. No. 138, ed. Stenflo, J.) 49-66 (Kluwer, Dordrecht, 1989).
14. November, L. J. *Astrophys. J.* **344**, 494-503 (1989).
15. Rand, J. & Huggins, M. C. R. *Acad. Sci. Paris* **249**, 625-627 (1959).
16. Simon, G. W. & Weiss, N. O. *Mon. Not. R. Astr. Soc.* **252**, 1p-5p (1991).
17. Busse, F. H. in *Hydrodynamic Instabilities and the Transition to Turbulence* (ed. Swinney, H. L. & Gollub, J. P.) 97-137 (Springer, Berlin) 1981.
18. Zocchi, G., Moses, E. & Lischke, A. *Physica A* **188**, 387-407 (1990).
19. Title, A. M. et al. *Astrophys. J.* **338**, 475-494 (1989).
20. Wang, Y.-M., Nash, A. G. & Sheeley, N. R. Jr. *Science* **245**, 717-718 (1989).